Electronic Supplementary Material (ESI) for Materials Chemistry Frontiers.

Supplementary Information

Covalent Organic Frameworks-based Nanoplatform with Enhanced Photothermal and Photodynamic Performance for Tumor Targeted Therapy

Chaoyu Wang[a], Zhihui Xin[a], Zhiqiang Bai[a,b], Jiaxin Mao[a], Yaru Li[b], Zhifang Jia[a], Kewei Wang[a], Lu Zhao[a*], Yunfeng Bai[a,b*], Feng Feng[a*]

[a] School of Chemistry and Chemical Engineering, Shanxi Provincial Key Laboratory of Chemical Biosensing, Shanxi Datong University, Datong 037009, China.

[b] School of Agriculture and Life Science, Shanxi Datong University, Datong 037009, China;

[*] Correspondence: cobra143@163.com (L ZHAO); baiyunfeng1130@126.com (Y BAI); feng-feng64@263.net (F FENG)

Experimental section

Materials and Reagents

All reagents were analytical grade and used without further purification. TAPB, DMTP, ICG, dimethyl sulfoxide (DMSO), acetonitrile, dopamine hydrochloride and ethanol were purchased from Shanghai Aladdin Biochemical Technology Co., Ltd. 1,3-Diphenylisobenzofuran (DPBF) was purchased from Adamas Reagent Co., Ltd. Roswell park memorial institute-1640 (RPMI-1640) medium, Dulbecco's modified eagle's medium (DMEM), phosphate-buffered saline (PBS) and trypsin-EDTA solution were purchased from Biosharp Reagent Co., Ltd. Fetal bovine serum (FBS) was obtained from Gibco Reagent Co., Ltd. 3-(4,5-Dimethyl-2-thiazolyl)-2,5-diphenyl-2H-tetrazolium bromide (MTT) and penicillin/streptomycin were purchased from Shanghai Sigma Aldrich Trading Co., Ltd. Calcein AM/PI cytotoxicity assay kit, Annexin V-FITC/PI apoptosis assay kit, ROS assay kit and Hoechst 33342 were acquired from Shanghai Beyotime Biotechnology Co., Ltd. Apt sequences (Table 1) were synthesized by Shanghai Sangon Biotech Co., Ltd.

Characterization

Scanning electron microscopy (SEM) images were recorded using MAIA3 microscope (TESCAN, Czech). The transmission electron microscopy (TEM) images, energy dispersive spectroscopy (EDS) and elemental mapping images were obtained using a JEM-2100F transmission electron microscope (JEOL, Japan). The ultraviolet-visible (UV-vis) absorption spectra of nanomaterials were recorded using a Lambda35 spectrometer (PerkinElmer, USA). Powder X-ray diffraction (PXRD) spectra of nanomaterials were measured on a Smart Lab SE diffractometer (Rigaku, Japan). All nanomaterials were scanned at a scanning rate of 5° min^{-1} in the 2θ range from 0.5° to 15° at room temperature. Fourier transform-infrared (FT-IR) spectra of nanomaterials were measured on a NICOLET iS20 Spectrometer (Thermo Scientific, USA). The Zeta sizer Nano ZS90 (Malvern Panalytical, UK) was used to determine the zeta potential and hydrodynamic size of the nanomaterials. Fluorescence spectra of nanomaterials were monitored by F-2500 fluorescence spectrometer (Hitachi, Japan). Photothermal performances of nanomaterials were detected and recorded using a 323pro infrared thermal imager (FOTRIC, China). The absorbance was measured in Infinite M200PRO microplate reader (TECAN, Switzerland) for the MTT assay. The confocal laser scanning microscopy (CLSM) images were recorded by an FV1200V inverted CLSM (Olympus, Japan). Flow cytometry experiments were conducted on a CytoFLEX flow cytometer (Beckman Coulter, USA).

Preparation of CIPA

Synthesis of COF. TAPB-DMTB COF (TD COF) was synthesized mainly according to a reported method[1]. The mixture of TAPB (9.84 mg), DMTP (8.16 mg) in acetonitrile (10 mL), acetic acid (40 μL) was stirred at 25℃ for 12 h. Then, the generated TD COF nanoparticles were isolated by centrifuging at 10,000 rpm for 6 min and washed thoroughly with acetonitrile and ethanol. After drying at 80°C for 12 h, TD COF was obtained as yellow crystalline powder.

Preparation of CI. TD COF (1.0 mg) was dispersed in 1.0 mL deionized water. ICG solution (0.5 mg mL^{-1}, 1.0 mL) was then added to the mixture followed by stir for 12 h. The product (CI) was collected through centrifugation and washed with deionized water for 3 times. In the meantime, the supernatant was collected and recorded the

absorbance at 779 nm to determine the amount of ICG in the solution. The ICG encapsulation efficiency (EE) could be calculated according to following formula (1):

$$EE\ (\%) = (m_{(initial\ ICG)} - m_{(unloaded\ ICG)})/m_{(initial\ ICG)} \times 100\% \quad (1)$$

Preparation of CP. TD COF (5 mg) was redisposed in 5 mL Tris-HCl buffer (pH 8.5, 10 mM) using ultrasound followed by addition of dopamine hydrochloride (5 mg). Then the mixture was stirred for 6 h. The product (CP) was collected by centrifugation and washed with deionized water for 3 times.

Preparation of CIP. CI (5 mg) was redispersed in 5 mL Tris-HCl buffer (pH 8.5, 10 mM) using ultrasound followed by addition of dopamine hydrochloride (5 mg). Then the mixture was stirred for 6 h. The product (CIP) was collected by centrifugation and washed with deionized water for 3 times.

Preparation of CIPA. Apt-A (2 OD) was dissolved in 500 μL Tris-HCl buffer (pH 8.5, 10 mM) and mixed with 1 mg of CIP. The mixture was stirred in the dark for 6 h to ensure sufficient reaction. The unbound Apt-A was removed by centrifugation (8000 rpm, 5 min) and the obtained product (CIPA) was washed with deionized water for 3 times. Apt-C was also modified on the CIP via the same method to construct CIPC as the control group.

Extracellular Photothermal and Photodynamic Effect

Photothermal Performance Evaluation.

The photothermal performances of different nanomaterials were recorded by monitoring their temperature variations under NIR laser irradiation. The photothermal properties of CIPA at different concentrations or different leaser power were investigated by using an infrared camera. The photostability was also evaluated by recording the temperature changes of CIP, CP and ICG aqueous solution for five laser on/off cycles.

Photothermal Conversion Efficiency.

The photothermal conversion efficiency of nanomaterials was determined based on the protocol reported before [2, 3]. First, the CI, CP CIP or CIPA aqueous solution was irradiated by 808 nm laser for 5 min (1.5 W cm^{-2}) and followed by a natural cooling period. Meantime, the temperature of solution was monitored every 10 s by infrared camera. The UV absorption spectra of different nanomaterials at 808 nm was measured via UV-vis spectrometer. The concentration of the product was calculated via Lambert-Beer law[4]. The photothermal conversion efficiency (η) was calculated by the following equation (2):

$$\eta = \frac{hS\Delta T_{max} - Q_{Dis}}{I(1 - 10^{-A_{808}})} \quad (2)$$

where η is the photothermal transfer coefficient, S is the surface area of the container, ΔT_{max} is the equilibrium temperature after 5 min irradiation, Q_{Dis} expresses the heat dissipation by the test cell, I is 808 nm laser power (1.2 W cm^{-2}), and A_{808} is the absorbance of the CI, CP, CIP or CIPA aqueous solution at 808 nm. The value of hS is determined according to the following equation (3):

$$hS = \frac{m_d C_d}{\tau_S} \quad (3)$$

that m_d is the mass (0.4 g) and C_d is the heat capacity (4.2 J g^{-1} ℃$^{-1}$) of the aqueous solvent, τ_S is the sample system time constant which is defined as the ratio of ΔT and ΔT_{max}. Where only τ_S is unknown in this equation for

calculation. In order to get the τ_S, we herein introduce ϑ:

$$\theta = \frac{\Delta T}{\Delta T_{max}} \quad (4)$$

$$t = -\tau_S(ln\theta) \quad (5)$$

Thus, τ_S can be determined by applying the linear time data from the cooling period versus – *ln* ϑ (equation 4, 5).

Substituting τ_S value into equation (2, 3), the η of different nanomaterials can be calculated.

Singlet Oxygen Detection.

TD COF, CI, CIP, CIPA (10 μL, 1.0 mg mL^{-1}) or ICG (166 μg mL^{-1}) was added to 1 mL DPBF (14 μg mL^{-1}) in DMSO solution. The UV-vis absorption spectra of the mixture were collected under NIR laser irradiation (808 nm, 1.5 W cm^{-2}).

Then the singlet oxygen produced by ICG and CIPA under laser irradiation was measured by singlet oxygen probe SOSG. The ICG (5 μL, 1 mg mL^{-1}) or CIPA (30 μL, 1 mg mL^{-1}) was mixed with 1μM SOSG aqueous solution (1 mL), and the fluorescence intensity of the mixture was measured every 1 min after the 808 nm laser irradiation (1.5 W cm^{-2}).

Intracellular Photothermal and Photodynamic Effect

Cell Culture and Cellular Uptake.

MCF-7 cells were incubated in RMPI 1640 medium with 10% FBS and 1% penicillin/streptomycin at 37°C in a humidified atmosphere containing 5% CO_2. HepG2 cells were cultured in DMEM with 10% FBS and 1% penicillin/streptomycin at 37 °C in a humidified incubator containing 5% CO_2. 1×10^5 MCF-7 cells were seeded into confocal dish. After attachment, cells were incubated with CIPA. Then the cells were stained by Hoechst 33342 for 15 min followed by washing 3 times with PBS and observing by CLSM.

Aptamer Affinity Analysis and Targeting Performance.

MCF-7 or HepG2 cells were collected and incubated with Apt-CF and Apt-AF for 2 h. Then, the cells were washed and resuspended in PBS, and the fluorescence intensity of the cells was assessed by flow cytometry.

In order to verify the targeting performance, MCF-7 or HepG2 cells were seeded in confocal dish or 6-well plates (1×10^5 cell per well) for 24 h. After attachment, cells were treated with CIPA (15 μg mL^{-1}), CIPA (15 μg mL^{-1}) + 2 OD Apt-C and CIPA (15 μg mL^{-1}) + 2 OD Apt-A. Then, cells were washed with PBS and analyzed by CLSM or flow cytometry.

Intracellular photothermal effect Test.

MCF-7 cells were seeded in 6-well plates. After incubation for 24 h, the cells were further incubated with various nanomaterials for 2 h. Subsequently, the MCF-7 cells were rinsed, collected and re-suspended in PBS. Then the cell suspension was irradiated while the temperature rise was recorded with an infrared thermal imager.

Intracellular Singlet Oxygen Detection.

2',7'-Dichlorodihydrofluorescein diacetate (DCFH-DA) was employed to detect the intracellular ROS generation. MCF-7 or HepG2 cells were seeded into confocal dish (1×10^5 cell per well). After attachment, cells were treated with different nanomaterials for 3 h. After that, cells were stained with DCFH-DA (10 μM) for 30 min and washed with PBS before irradiated. Then the green fluorescence signal was captured by CLSM.

Biocompatibility Assay.

The biosafety of nanomaterials was detected by MTT method. Briefly, MCF-7 or HepG2 cells were seeded in 96-well plates (5×10^4 cells per well) for 24 h. Then, different concentrations of TD COF or CIPA were added to the wells and incubated with the cells for 24 h. Then the cells were washed with PBS and incubated with fresh medium containing MTT for 4 h. Subsequently, the supernatant was discarded and 150 μL DMSO was added. The absorbance was recorded at 570 nm with a microplate reader using untreated cells as controls.

Cell Cytotoxicity Assay.

MCF-7 or HepG2 cells were seeded into 96-well plates (5×10^4 cell per well). After 24 h, different nanomaterials were added to the wells and incubated with the cells for 3 h. Subsequently, the cells were washed with PBS, and all the laser-involved groups were exposed to 808 nm laser irradiation. Then, the cell viability was detected by MTT method after cultured for another 12 h.

Live/Dead Cell Staining Assay.

MCF-7 or HepG2 cells were cultured in medium containing different nanomaterials (200 μg mL^{-1}) for 3 h, and then irradiated with 808 nm laser (1.5 W cm^{-2}) for 10 min. These living and dead cells were then incubated for 30 min in Calcein-AM/PI staining solution. The fluorescence images of cells were obtained with CLSM.

Hemolysis Assay.

1.0 mL of PBS, H_2O and different concentrations (50, 100 and 200 μg mL^{-1}) of TD COF or CIPA in PBS solutions were mixed with 4% erythrocytes (v/v, 1.0 mL). After incubation at 37°C for 4 h, the supernatant was collected by centrifugation (3000 rpm, 3 min), and the absorbance at 570 nm was measured using a microplate reader.

In vivo Tumor Therapy

All mice experiments were performed under the permission of experimental animal ethics committee of Shanxi Datong University. 4 weeks-old female nude Balb/c mice were obtained from Beijing Weitonglihua Biotechnology Co., Ltd. The tumor model was established by subcutaneously injecting MCF-7 cells (8×10^6 cells) into the groin region of mice. After the tumor size reached ~100 mm^3, the tumor-bearing mice were randomly divided into six groups for different treatments: (1) PBS, (2) CP + laser, (3) CI + laser, (4) CIP + laser, (5) CIPC + laser and (6) CIPA + laser. Correspondingly, the experimental mice were intravenously injected with different nanomaterials (2 mg mL^{-1}, 0.1 mL). After 4 h, the tumor site of mice was exposed to 808 nm laser for 6 min for irradiation groups. During irradiation, the temperature rise of different groups mice were recorded with an infrared thermal imager. The tumor size and body weight of experimental mice were monitored every two days and calculated as $V = length \times width^2/2$. After 17 days of treatment, the tumor tissues were sectioned into slices and stained with hematoxylin-eosin (H&E), TDT-mediated dUTP nick-end labeling (TUNEL) and Ki-67 for histological analysis. The main organs (heart, lung, liver, spleen and kidney) of the mice were collected and evaluated by H&E staining.

Statistical Analysis

SPSS 21.0 software was used for data analysis. One-way analysis of variance was used to compare the statistical analysis. Statistical significance was defined as: * $P < 0.05$, ** $P < 0.01$ and *** $P < 0.001$.

Table 1. Apt sequences in this work.

Name	Sequences (5'-3')
Apt-A	NH_2-$(CH_2)_6$-GCA GTT GAT CCT TTG GAT ACC CTG GTT TTT TTT TT
Apt-C	NH_2-$(CH_2)_6$-ATT GCA CTT ACT ATA TTG CAC TTA CTA TAT TGC AC
Apt-AF	NH_2-$(CH_2)_6$-GCA GTT GAT CCT TTG GAT ACC CTG GTT TTT TTT TT-FAM
Apt-CF	NH_2-$(CH_2)_6$-ATT GCA CTT ACT ATA TTG CAC TTA CTA TAT TGC AC-FAM

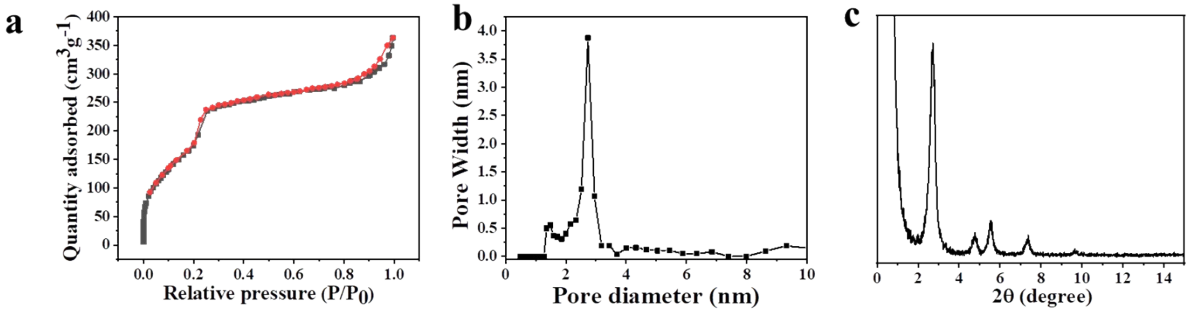

Fig. S1 (a) N_2 adsorption-desorption isotherm, (b) pore size distribution and (c) PXRD pattern of TD COF.

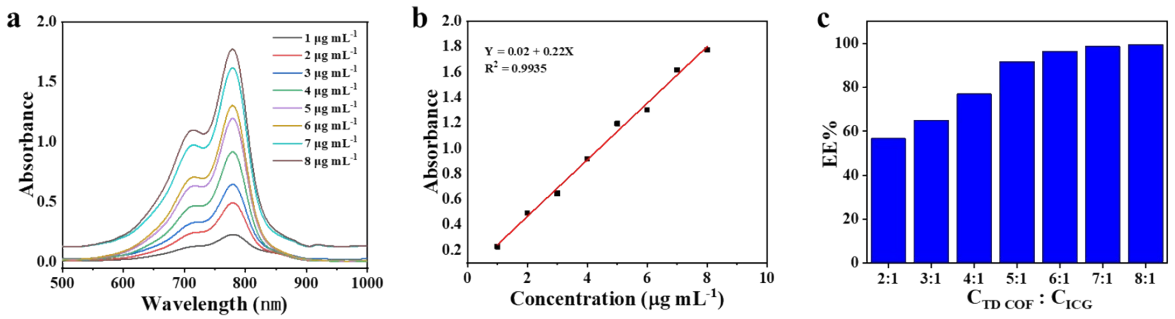

Fig. S2 (a) UV-vis spectra of ICG at different concentrations. (b) The standard curve of ICG at 808 nm. (c) Encapsulation efficiency of ICG in different proportions of TD COF and ICG.

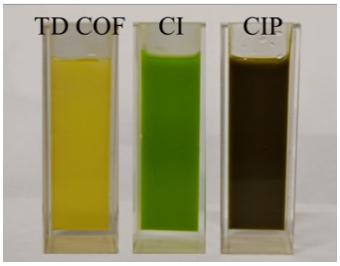

Fig. S3 The photograph of TD COF, CI and CIP in PBS.

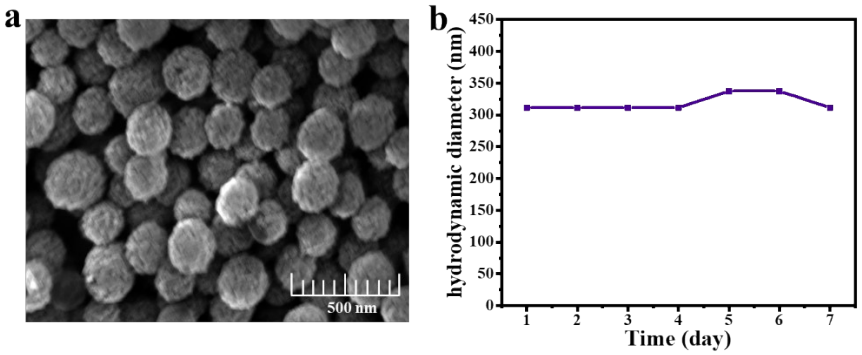

Fig. S4 (a) SEM image of CIPA. (b) Hydrodynamic diameter of CIPA in pH 7.4 PBS solutions.

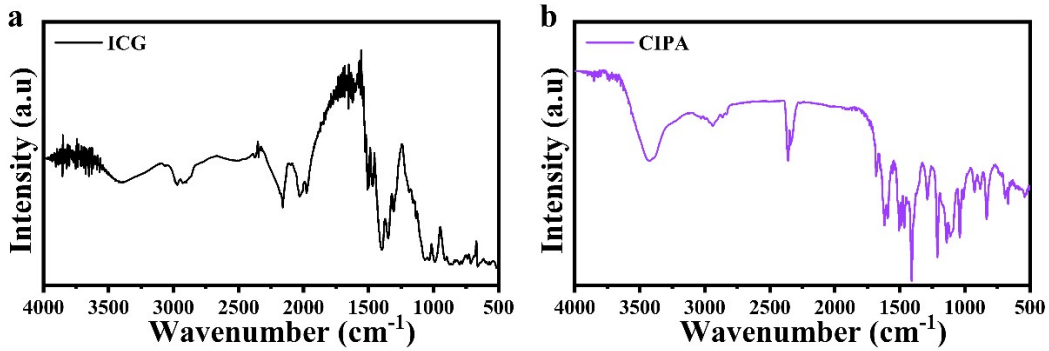

Fig. S5 The FT-IR spectrum of (a) ICG (b) and CIPA.

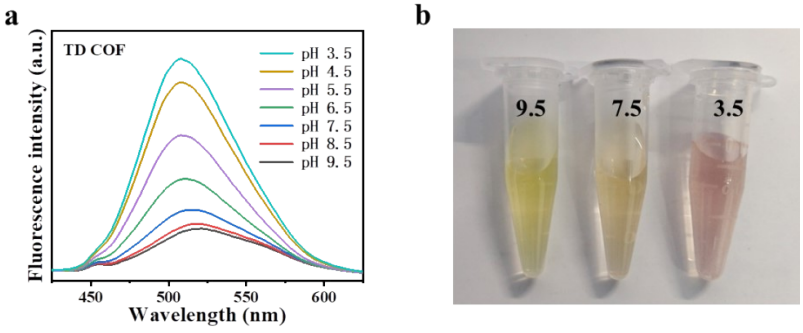

Fig. S6 (a) The fluorescence spectra of TD COF in PBS with different pH values. (b) The photograph of TD COF in PBS with different pH values.

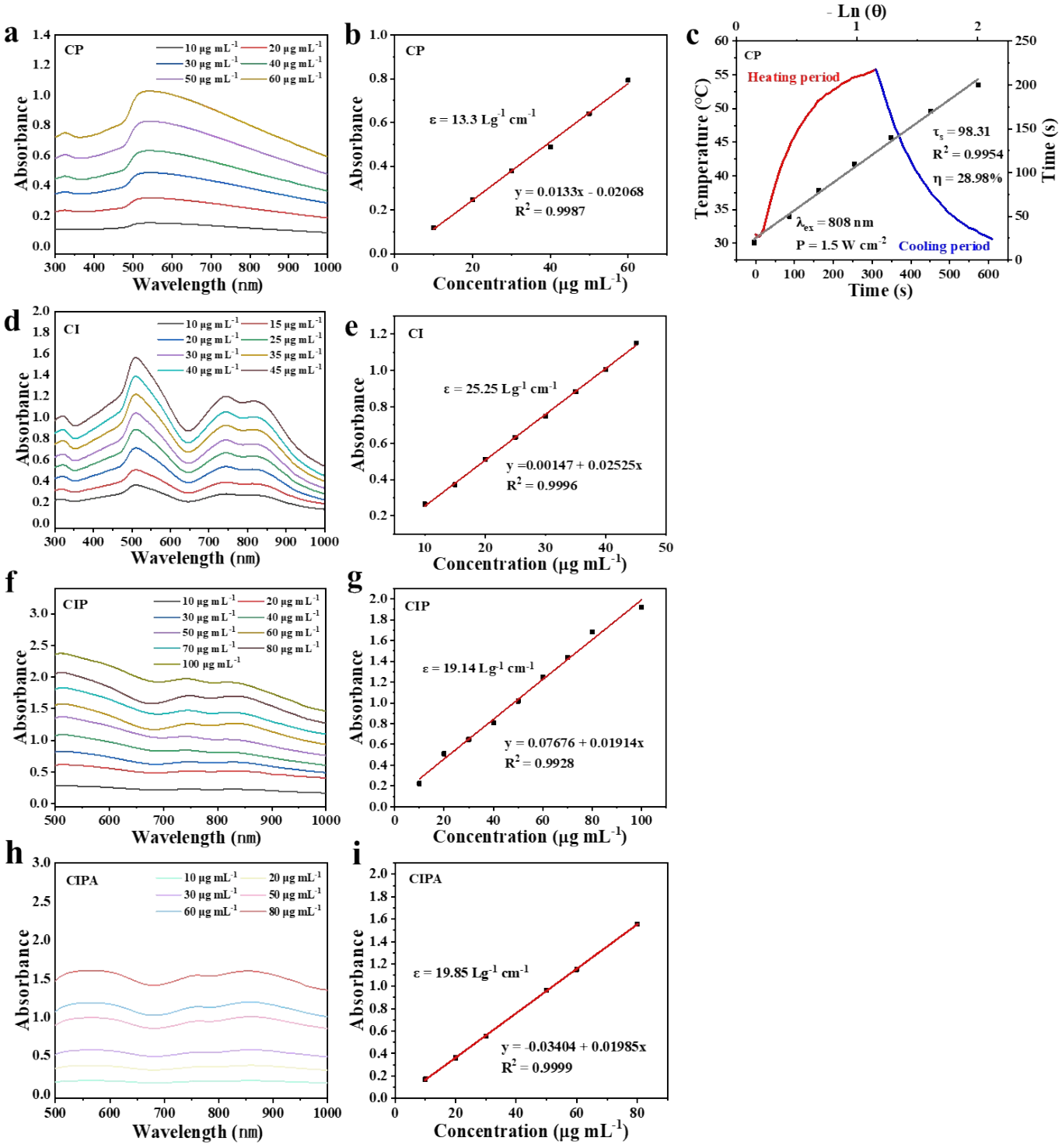

Fig. S7 UV-vis spectra of (a) CP, (d) CI, (f) CIP and (h) CIPA with different concentrations. Mass extinction coefficient of (b) CP, (e) CI, (g) CIP and (i) CIPA at 808 nm. (c) Calculation of time constant and photothermal conversion efficiency of CP dispersed in aqueous solution under 808 nm laser irradiation.

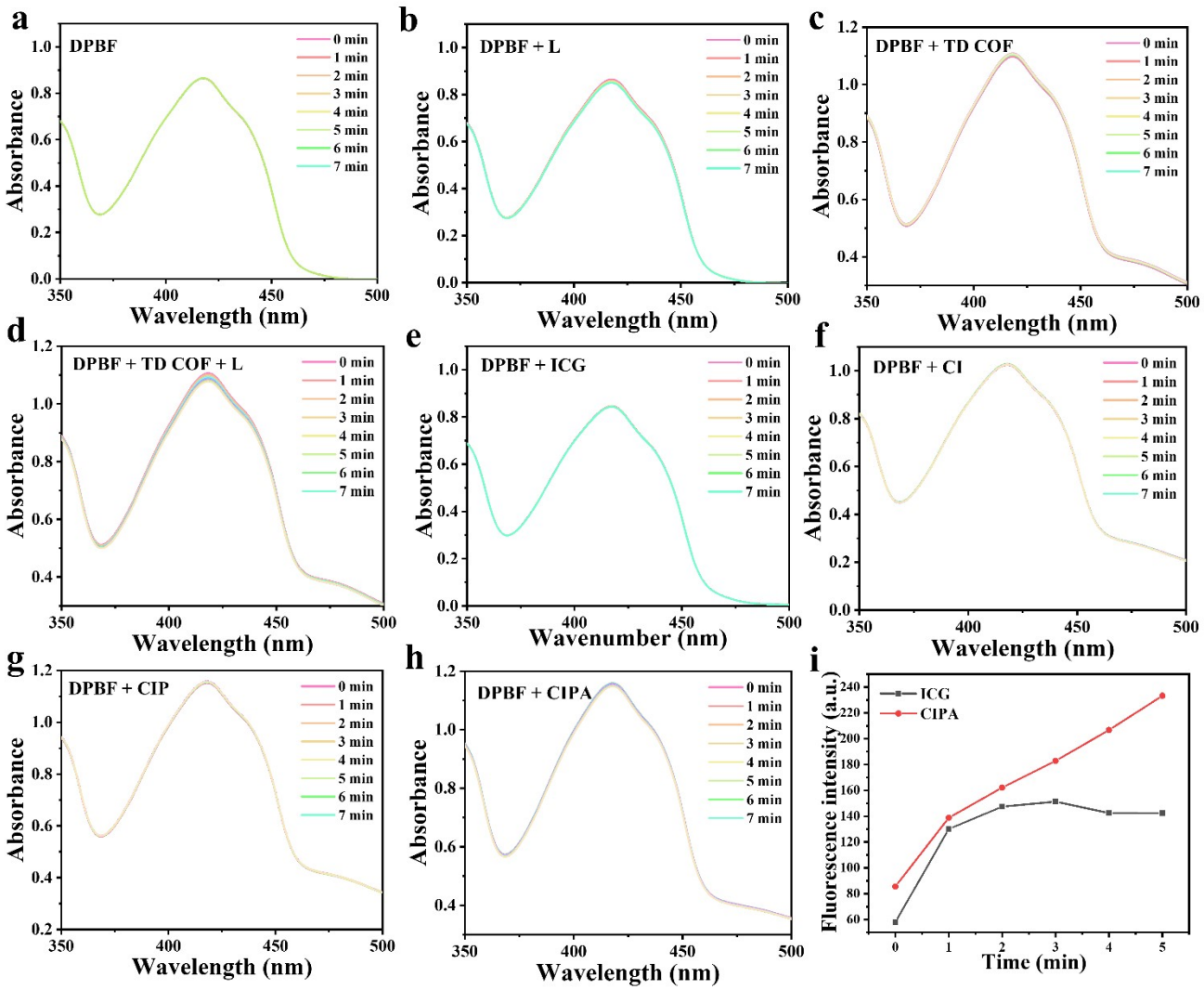

Fig. S8 UV-vis spectra of (a) DPBF, (b) DPBF + laser (L), (c) DPBF + TD COF, (d) DPBF + TD COF+ L, (e) DPBF + ICG, (f) DPBF + CI. (g) DPBF + CIP and (h) DPBF + CIPA. Laser involved groups were exposed to 808 nm laser at 1.5 W cm^{-2}. (i) A SOSG probe was used to determine $^1O_2$ by ICG and CIPA under laser irradiation.

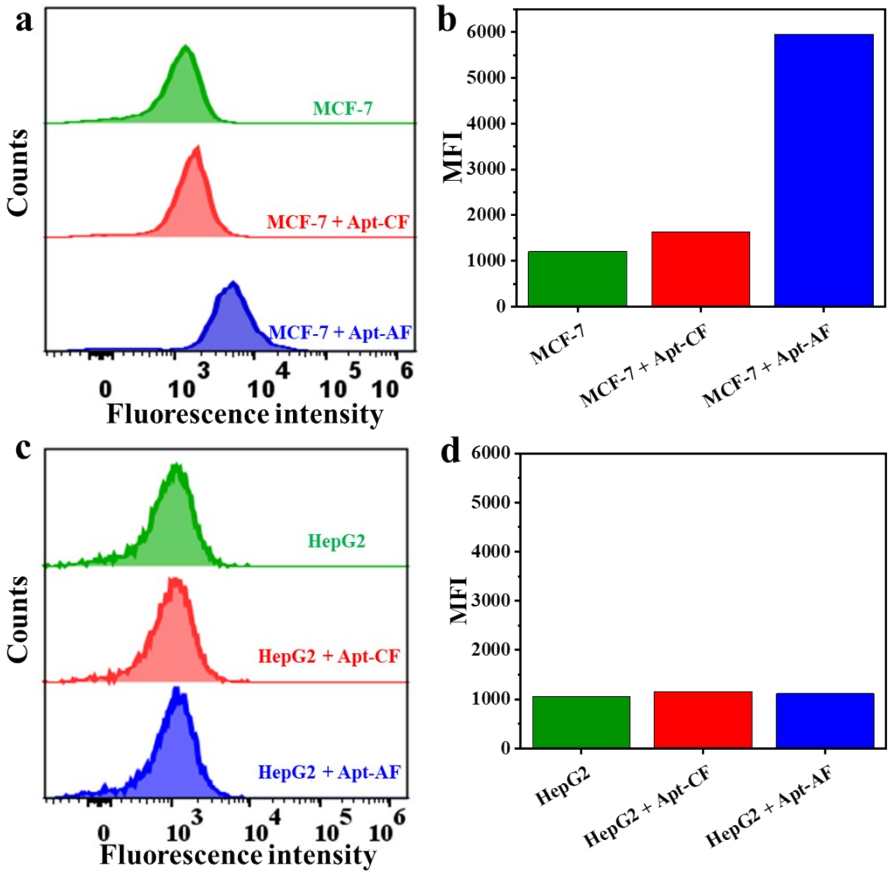

Fig. S9 Flow cytometric analysis of (a, b) MCF-7 and (c, d) HepG2 cells after incubated with Apt-AF and Apt-CF.

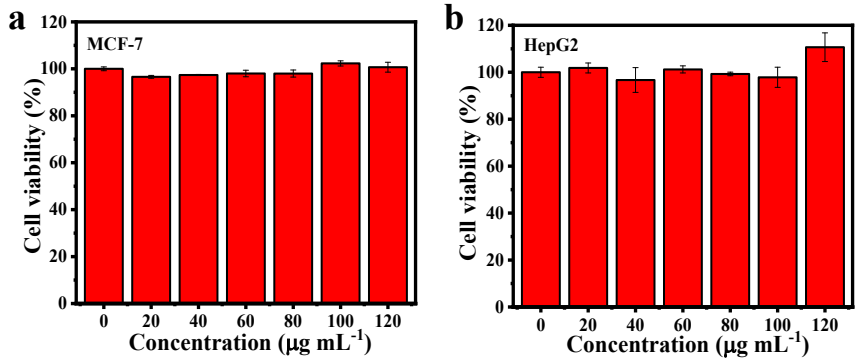

Fig. S10 The cell viability of (a) MCF-7 and (b) HepG2 cells after treatment with TD COF with various concentrations for 24 h.

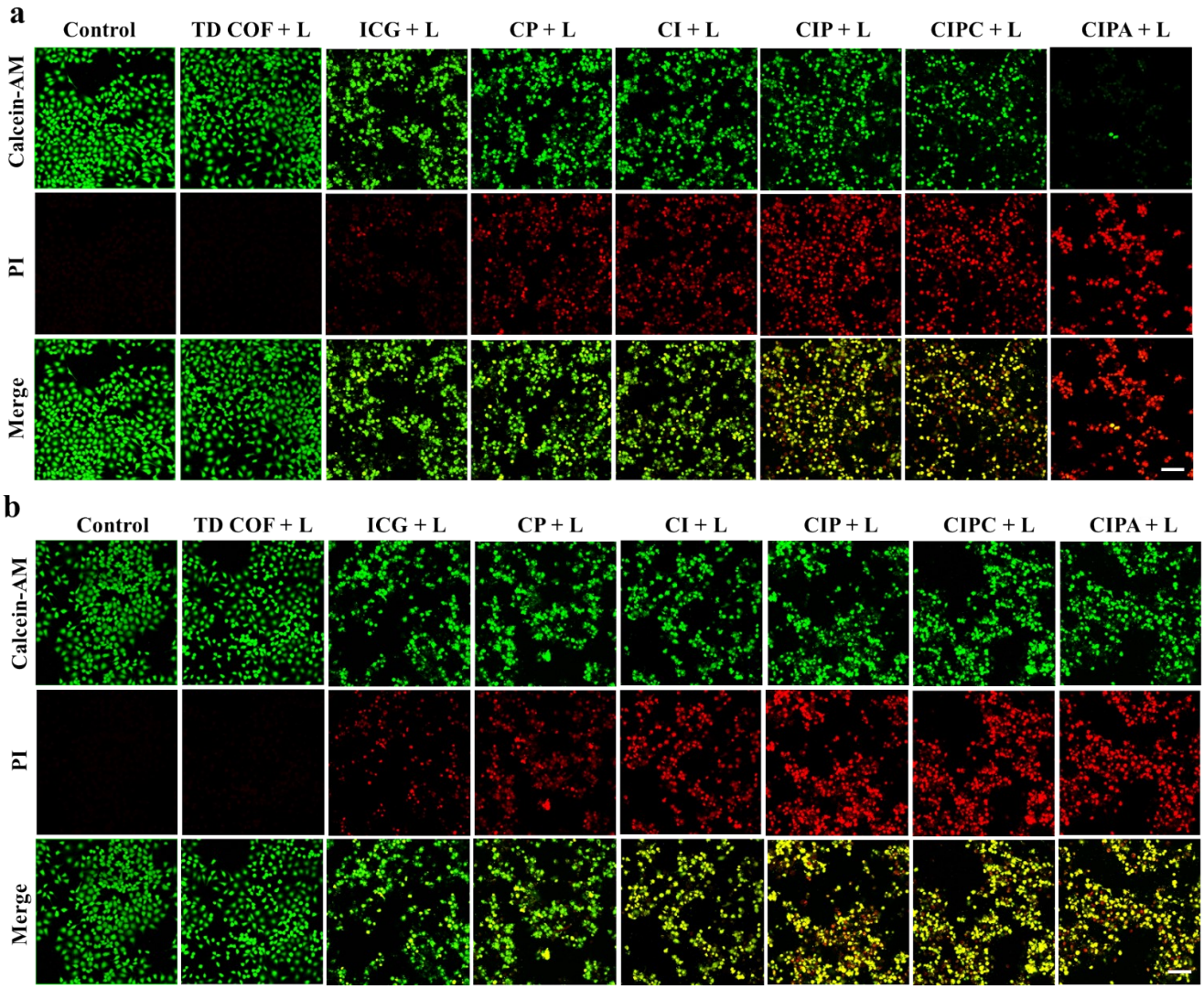

Fig. S11 CLSM images of (a) MCF-7 and (b) HepG2 cells after various treatments followed by Calcein-AM (green fluorescence) and PI (red fluorescence) staining. Scale bar: 100 μm.

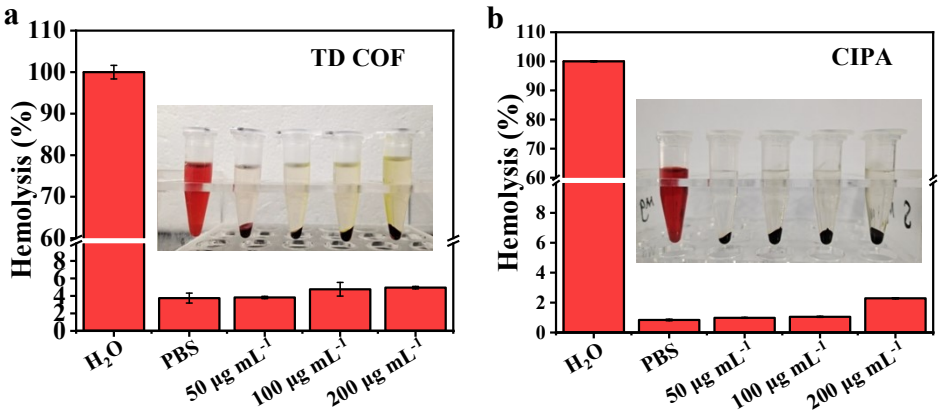

Fig. S12 Hemolysis detection of (a) TD COF and (b) CIPA at various concentrations.

Fig. S13 Representative digital photographs of tumor-bearing mice after different treatments.

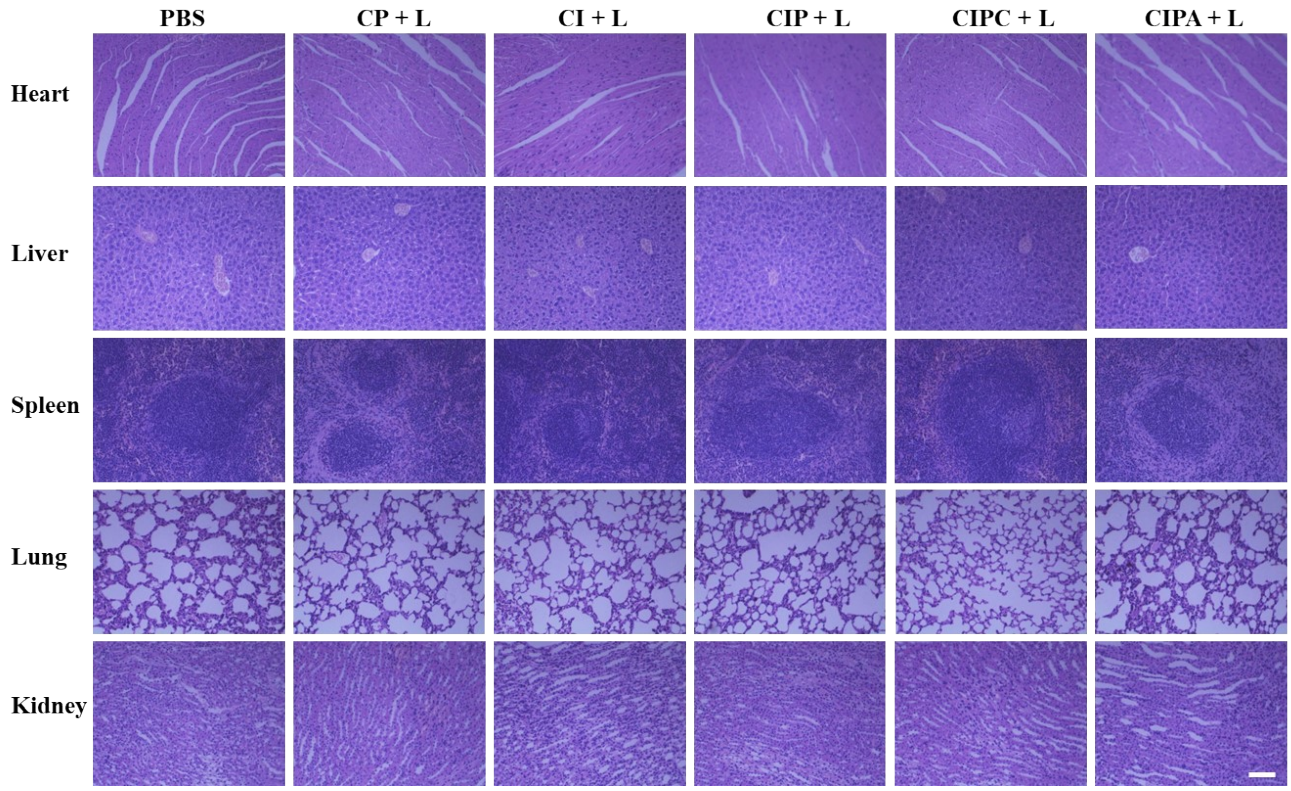

Fig. S14 Images of H&E stained main organs (heart, liver, spleen, lung and kidney) with different treatments. Scale bar: 100 μm.

References

[1] Q. Guan, L.L. Zhou, Y.A. Li, W.Y. Li, S.M. Wang, C. Song, Y.B. Dong, ACS Nano, 13 (2019) 13304-13316.

[2] X. Chen, F. Li, R. Liang, W. Liu, H. Ma, T. Lan, J. Liao, Y. Yang, J. Yang, N. Liu, ACS Appl. Mater. Interfaces, 15 (2023) 16343-16354.

[3] Y. Zhou, S.N. Liu, C.L. Hu, L.H. Cai, M.L. Pang, J. Mat. Chem. B, 8 (2020) 5451-5459.

[4] D.K. Roper, W. Ahn, M. Hoepfner, The Journal of Physical Chemistry C, 111 (2007) 3636-3641.